Studies of high temperature sliding wear of metallic dissimilar interfaces

INMAN, I. A., DATTA, P. K., DU, H. L., BURNELL-GRAY, J. S., PIERZGALSKI, S. and LUO, Q. <http://orcid.org/0000-0003-4102-2129>

Studies of high temperature sliding wear of metallic dissimilar interfaces

I.A. Inman[a]*, P.K. Datta[a], H.L. Du[a], J.S. Burnell-Gray[a], S. Pierzgalski[a], Q. Luo[b]

[a]Advanced Materials Research Institute, Northumbria University, Newcastle upon Tyne NE1 8ST, UK

[b]Materials Research Institute, Sheffield Hallam University, Sheffield S1 1WB, UK

Abstract: The evolution of microstructures in the glaze layer formed during limited debris retention sliding wear of Nimonic 80A against Stellite 6 at 750 8C and a sliding speed of 0.314 m s^{-1} (7 N applied load, 4522 m sliding distance) was investigated using scanning electron microscopy (SEM), energy dispersive analysis by X-ray (EDX), X-ray diffraction (XRD), scanning tunnelling microscopy (STM) and transmission electron microscopy (TEM). The collected data indicate the development of a wear resistant nano-structured glaze layer. The process of 'fragmentation' involving deformation, generation of dislocations, formation of sub-grains and their increasing refinement causing increasing misorientation was responsible for the formation of nano-structured grains. The rapid formation of this glaze layer from primarily cobalt–chromium debris transferred from (and also back to) the surface of the Stellite 6, kept wear of both the Nimonic 80A and Stellite 6 to very low levels.

However, increasing the sliding speed to 0.905 m s^{-1} (750 °C) suppressed glaze formation with only a patchy, unstable glaze forming on the Stellite 6 counterface and an absence of glaze development on the Nimonic 80A sample (the Nimonic 80A surface was covered with at most, a very thinly smeared layer of oxide). The high levels of oxide debris generated at 0.905 m s^{-1} instead acted as a loose abrasive assisting wear of especially the Nimonic 80A. This behaviour was attributed to a change in oxide chemistry (due to the dominance of nickel and chromium oxides generated from the Nimonic 80A) resulting in poor oxide sintering characteristics, in combination with increased mobility and reduced residency of the oxide debris at 0.905 m s^{-1}.

Key Words: High temperature wear; Dissimilar materials; Nano-scale; Glaze layer; Oxidation

1. Introduction

High temperature wear is a serious problem in many situations, typical examples including power generation, transport, materials processing and turbine engines [1–5]. The problem of high temperature wear is accentuated due to faster kinetics of surface oxidation, loss of mechanical hardness and strength of the materials that form the contacting surfaces and changes in adhesion between these surfaces caused by the joint action of temperature and tribological parameters. Efforts to prevent wear have included the use of oxidation resistant and thermally stable materials and also coatings and materials with preoxidised surfaces [1–8]. However, the conditions associated with high temperature environments severely restrict the choice of coatings and materials that can be used to prevent or minimise high temperature wear [1–3].

An alternative method of generating wear resistant surfaces on coated and uncoated materials is to take advantage of some of the important events accompanying the process of high temperature wear, such as oxidation, debris generation and elemental transfer between the contacting surfaces [1–3,9]. These events under certain conditions of temperature, pressure and speed led to the formation of glazes on the contacting surfaces, which can provide enhanced resistance to further wear [1–3,9–18]. Although the phenomenon of glaze formation and the general issues relating to wear at elevated temperatures have been extensively studied [1–3,9–18], it is still difficult to predict the precise conditions which promote the formation of glazed surfaces. A step forward would be to gain detailed knowledge of the micro-scale and nano-scalestructures of these layers, so that the mechanisms of glaze layer formation can be established. This project on high temperature wear was initiated with this objective in mind. This paper summarises and updates the studies carried out on glaze layers formed during the wear of Nimonic 80A as a sample material versus a Stellite 6 counterface at 750 °C and 0.314 m s^{-1} conducted within AMRI [3,19].

The effect of increasing the sliding speed to 0.905 m s^{-1} (and hence increasing debris mobility and reducing debris residency and retention) on the formation of these glaze layers is also investigated.

2. Experimental

The compositions of sample (Nimonic 80A) and counterface (Stellite 6) materials used for the experimental work are detailed in Table 1.

All wear tests were carried out on a high temperature ‘reciprocating-block-on-rotating-cylinder’ wear rig in open air, as shown in Fig. 1—such a configuration tends not to encourage debris retention. Details of the high temperature wear machine used have been previously described [1–

Table 1 Nominal compositions of alloys (in at.%)

	Ni	Cr	Ti	Al	Fe	Si	C	Co	W	Mn

Nimonic 80A	75.8	19.4	2.5	1.4	1.7	0.1	0.08	-	-	-
Stellite 6	<2.5	27	-	-	<2.5	1	1	60	5	1

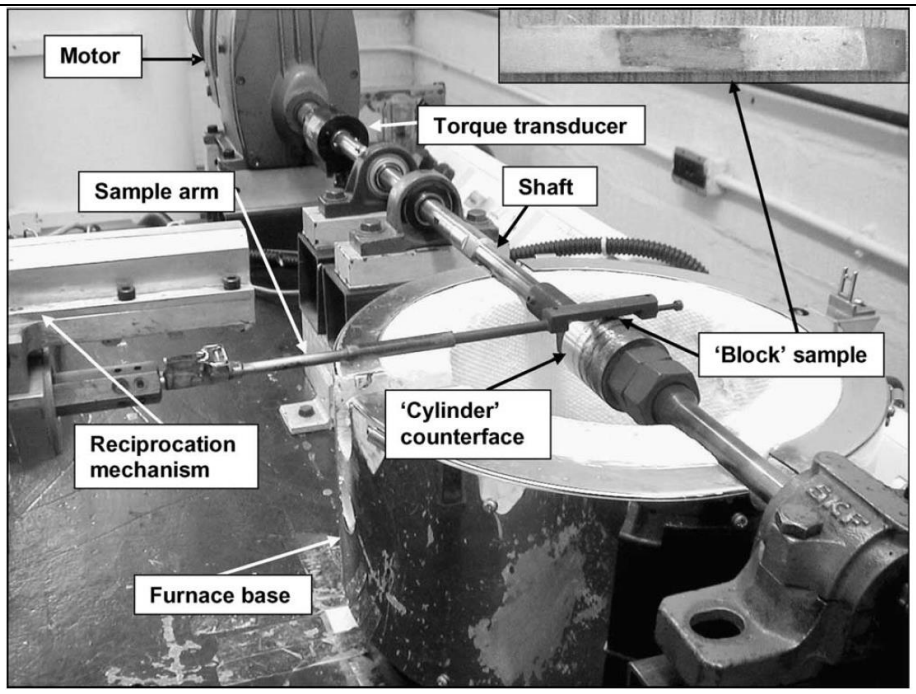

Fig. 1. Reciprocating high temperature block-on-cylinder wear rig, as used in the current experimental programme, plus a 'block' sample used during sliding experiments (shown example with glaze layer formed by sliding at 0.314 m sK1 and 750 8C).

3] (the block forming the sample and the cylinder being the counterface). A variable speed electric motor rotated the shaft and connected counterface (Stellite 6) of diameter 50 mm and length 50 mm at various speeds. Cleaned samples of Nimonic 80A polished to a 1 mm surface finish and of dimensions 5 mm!5 mm!45 mm were held against the counterface (polished to a 1200 grit surface finish and also cleaned) using a sample arm in reciprocating motion, with reciprocation at 3 cycles per minute and a constant stroke of 12 mm. The tests were carried out at sliding speeds of 0.314 and 0.905 m s^{-1} (representing different speeds of rotation at the surface of the counterface), under a load of 7 N at various temperatures between room temperature and 750 °C—the current studi s focus on the situation at 750 °C. The total sliding distance for all tests was 4522 m.

A minimum of three sliding tests (one test per sample) were conducted for each combination of test conditions - the weight of each sample was measured using a high accuracy Sartorious microbalance before and after sliding, from which a mean weight change value for each combination of sliding speed and temperature was calculated. The wear of the Stellite 6 counterface was briefly examined and not assessed quantitatively in this study—this is discussed in more detail elsewhere [3].

A Melbourne type TRP-50 torque transducer connected to the wear rig's rotating counterface shaft collected the coefficient of friction data.

The surface layers produced at 0.314 m s^{-1} and 750 °C were characterised at two levels as described by Inman et al. [3,19]. The evolution of the microstructures generated was characterised at the micro-scale level using scanning electron microscopy (SEM), energy dispersive analysis by X-ray (EDX) and X-ray diffraction analysis (XRD). Nanoscale information on the surface layers produced at 0.314 m s^{-1} was obtained using mainly transmission electron microscopy (TEM) and also scanning tunneling microscopy (STM).

Nano-indentation tests were additionally carried out on glaze layers formed on four Nimonic 80A samples slid against a Stellite 6 counterface at 0.314 m s^{-1} and 750 °C (discussed previously [3]), using a Hysitron nano-indenter with a 150 nm Berkovich three-sided pyramidal indenter. The test time in each case was 10 s, with a 5 s ramp up period to maximum load and 5 s ramp down period back to zero load. The maximum load used was 5000 mN unless otherwise stated—this was the highest load possible without the indenter penetrating the glaze layer. The wear surfaces produced at 750 °C and 0.905 m s^{-1} could only be characterised at micro-scale level using SEM, EDX and XRD, due to a lack of surface deposits and an uneven surface profile. Nano-scale characterisation was not feasible.

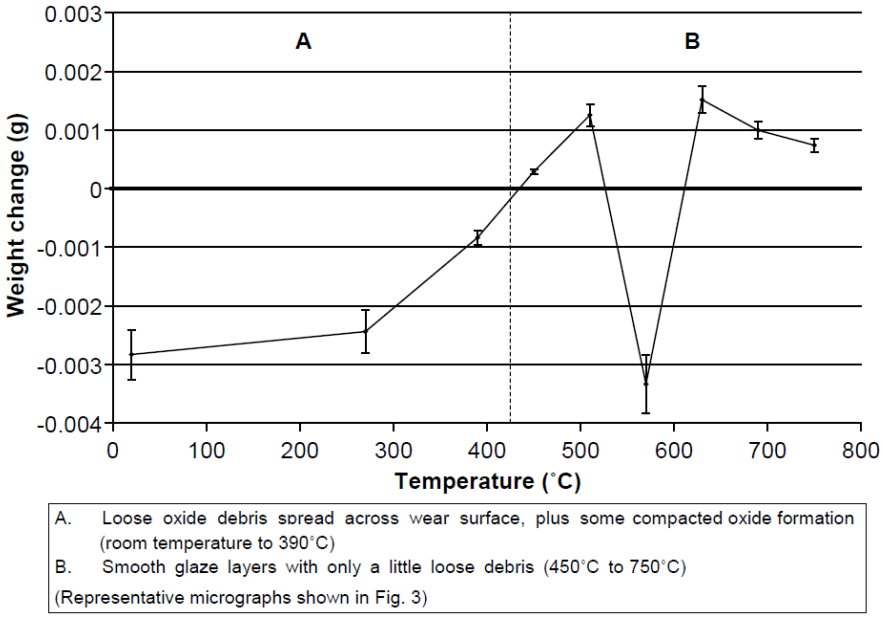

Fig. 2. Weight change versus temperature for Nimonic 80A slid against Stellite 6 at 0.314 m s^{-1}.

3. Results

3.1. Wear at 0.314 m s^{-1}

3.1.1. General observations—room temperature to 750 °C

Fig. 2 displays the wear data for the Nimonic 80A (sample)/Stellite 6 (counterface) system as a function of temperature under a load of 7 N at 0.314 m s^{-1} for a total sliding distance of 4522 m. Weight changes were extremely low for all temperatures—very slight losses were recorded (indicated by negative weight change values) at room temperature (mean Nimonic

80A sample weight change K0.002(8) g) and 270 °C (weight change K0.002(4) g), with a negligible weight lossobserved at 390 °C. These slight sample weight losses coincided with the presence of loose oxide debris (of size 300 nm to 1 mm) and some areas of compacted oxide on the wear scar

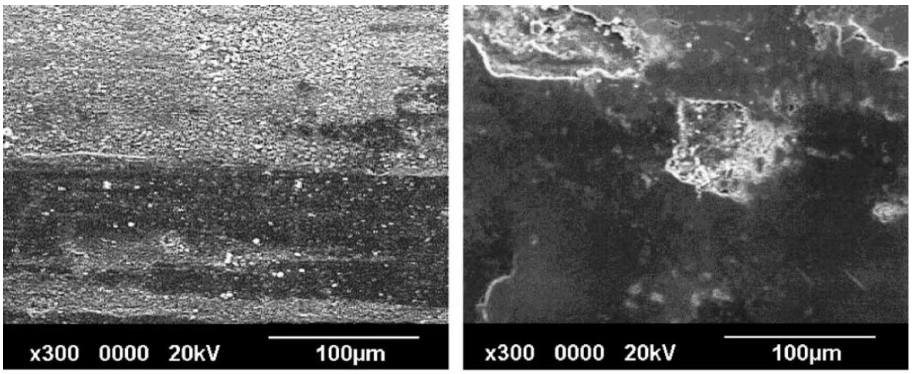

A Loose oxide, plus some compacted oxide layers – room temperature (shown example) to 390°C

B Smooth glaze layer formation with little debris – 510°C to 750°C (shown example)

Fig. 3. SEM images of Nimonic 80A wear surfaces after sliding at 0.314 m s-1 against a Stellite 6 counterface at room temperature and 750 °C.

surfaces of both the Nimonic 80A sample (Fig. 3) and Stellite 6 counterface (not shown).

Slight weight gains were observed for the Nimonic 80A samples at all test temperatures between 450 (negligible weight gain) and 750 °C (weight change 0.000(7) g), with the highest mean weight change values at 510, 630 and 690 °C of 0.001(1), 0.001(4) and 0.001(0) g, respectively (Fig. 2). These sample weight gains coincided with the formation of definite glaze layers on the wear scar surfaces of both sample (Fig. 3) and counterface (not shown).

The very low levels of wear damage on both the Nimonic 80A sample and the Stellite 6 counterface were directly attributable to the presence of the loose oxide debris and compacted oxide between room temperature and 390 °C and the glaze layers between 450 and 750 °C. The presence of the oxide in debris or glaze form prevented metal-to-metal contact and severe wear by metallic adhesion [3].

The weight loss data at 570 °C (weight change K0.003(3) g) shows a departure from the general trend of positive weight change (i.e. weight gain) between 510 and 750 °C—further testing confirmed the weight loss data at 570 °C (eight repeat experiments were conducted), indicating that the wear process needs further attention at this temperature. However, this paper concentrates on the situation at 750 °C.

3.1.2. Wear at 750 8C (0.314 m s^{-1})

Measurement of coefficient of friction values at 750 °C and 0.314 m s^{-1} showed a brief unsettled ‘run-in’ period of increased friction (as high as ~0.7) and rapid change at the very beginning of testing, before settling down into a ‘steady state’ with reduced variation (between 0.47 and 0.55). The measured coefficients of friction in Fig. 4 show no significant changes with time after this initial unsettled period. The very brief run-in period indicates that the onset of the

formation of a glaze layer was almost immediate—the lack of variation after this initial peak in friction during the 'steady state' phase was due to the continued presence of the glaze on the worn surface.

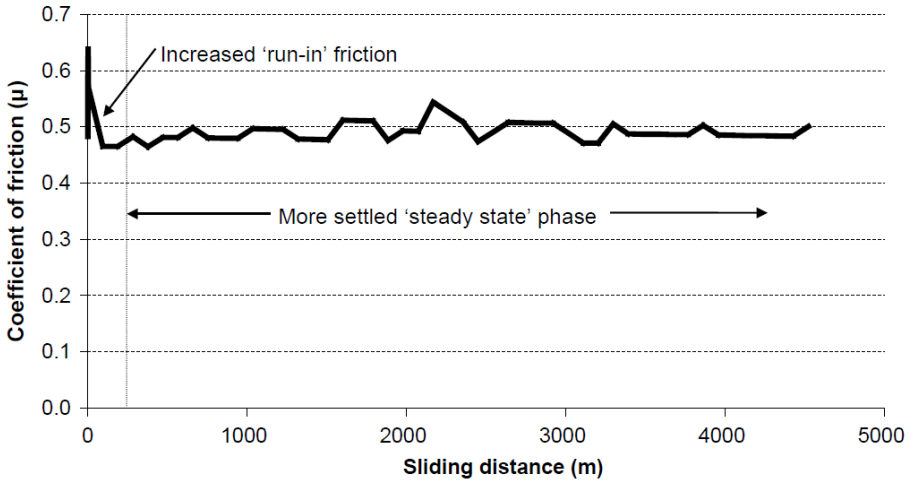

Fig. 4. Coefficient of friction versus time for Nimonic 80A versus Stellite 6 at 0.314 m s^{-1} and 750 °C.

EDX analysis of the oxide glaze layers generated on the Nimonic 80A after sliding for 4522 m at 750 °C indicated the dominance of Co (34.2 at.%), Cr (36.2 at.%) and Ni (16.7 at.%), with Si (3.8 at.%) and Fe (1.3 at.%) also present as trace elements. This indicated that although there was a high degree of transfer from the Stellite 6 counterface to form the Co–Cr dominated glaze layer, some intermixing of material from the Nimonic 80A as the sample (as indicated by the presence of Ni) also occurred. The presence of these elements was also confirmed by TEM EDS, which showed some location-to-location variation. The dominant phases identified by XRD were CoCr2O4 (within the glaze layer) and a face centred cubic Ni–Cr–Fe pattern typical of the Nimonic 80A forming the sample.

Fig. 5 illustrates a cross-sectional composite transmission electron micrograph of the surface formed during wear testing at 750 °C. The micrograph demonstrates the presence of the surface glaze layer, the deformed substrate and the glaze layer/substrate interface. The wear-affected region consisted of a number of sub-layers—the topmost 1 mm of the 3.5 mm thick glaze layer showed the presence of uniform grain structure of size 5–15 nm; some of the grains displaying contrast—the dislocation density in this area was low. The lower 2.5 mm of the glaze layer and the interfacial zone consisted of grains of size 10–20 nm and had a higher dislocation density. The Nimonic 80A metallic substrate just beneath the interfacial zone showed subsurface deformation and the presence of elongated grains.

The structure of the glazed layer and the selected analysis diffraction (SAD) pattern are separately presented in Fig. 6. The SAD pattern consisted of spots arranged in concentric circles that indicated the presence of small grains with high angle boundaries, multiple boundaries and large misorientations (formation of misorientated lattice-fragmentation). The poorly defined irregular boundaries indicate a non-equilibrium high-energy configuration. The

indexed SAD pattern (not shown) also revealed the presence of oxides of Ni, Cr and Co. The dark field images further elaborate on the grain structure of the glaze layer.

The occurrence of sub-surface deformation is also illustrated in Fig. 5. Dislocations have been observed in the deformed substrate. These dislocations were present as networks inside

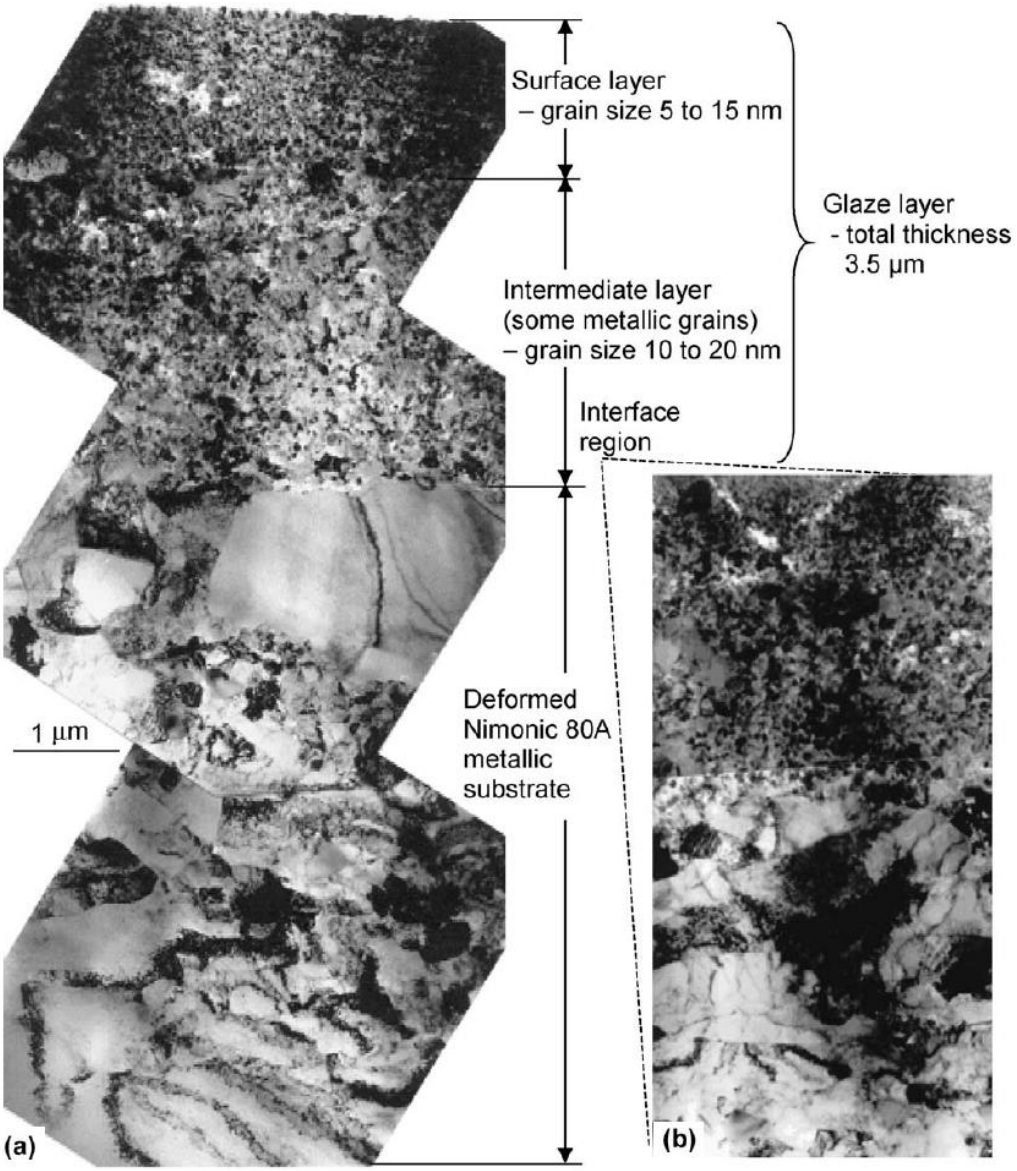

Fig. 5. Nano-scale characterisation of glaze layers formed at 0.314 m sK1 and 750 8C showing TEM bright field images of (a) a wear-induced polycrystalline glaze layer plus substrate deformation and (b) the interface of the glaze layer and deformed substrate.

the deformed (elongated) grains. It was evident that shearing deformation took place in the substrate as a response to the sliding process.

Table 2 Nano-indentation data for glaze layers formed on Nimonic 80A slid against Stellite 6 at 0.314 m s^{-1} and 750 °C

	Sample 1	Sample 2	Sample 3	Sample 4	Mean
Nominal load (μN)	5000	5000	5000	1000	–
Actual load (μN)	4968.4	4967.8	4964.1	996.4	–
Hardness (GPa)	24.50	27.34	16.62	22.01	22.62
Modulus (GPa)	130.2	131.1	110.4	147.1	129.7

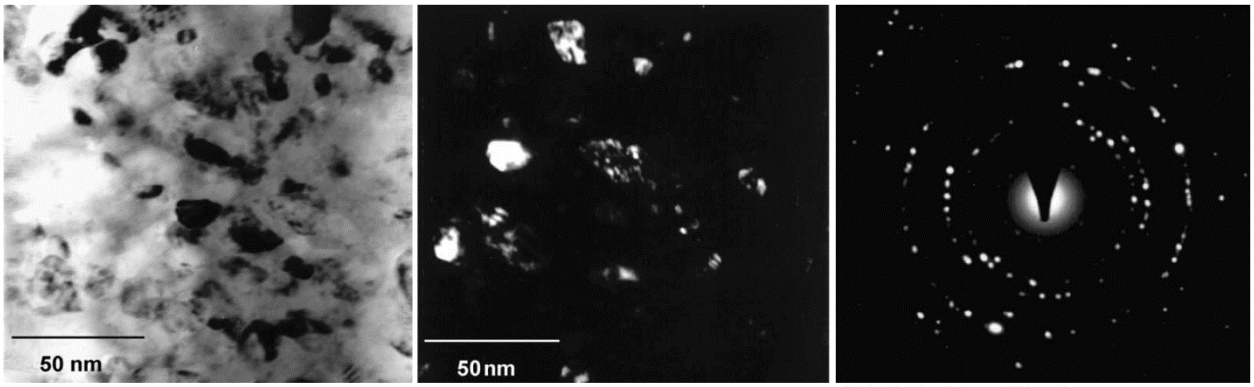

Fig. 6. TEM morphological and structural details of the glaze layer formed at 0.314 m s^{-1} and 750 °C.

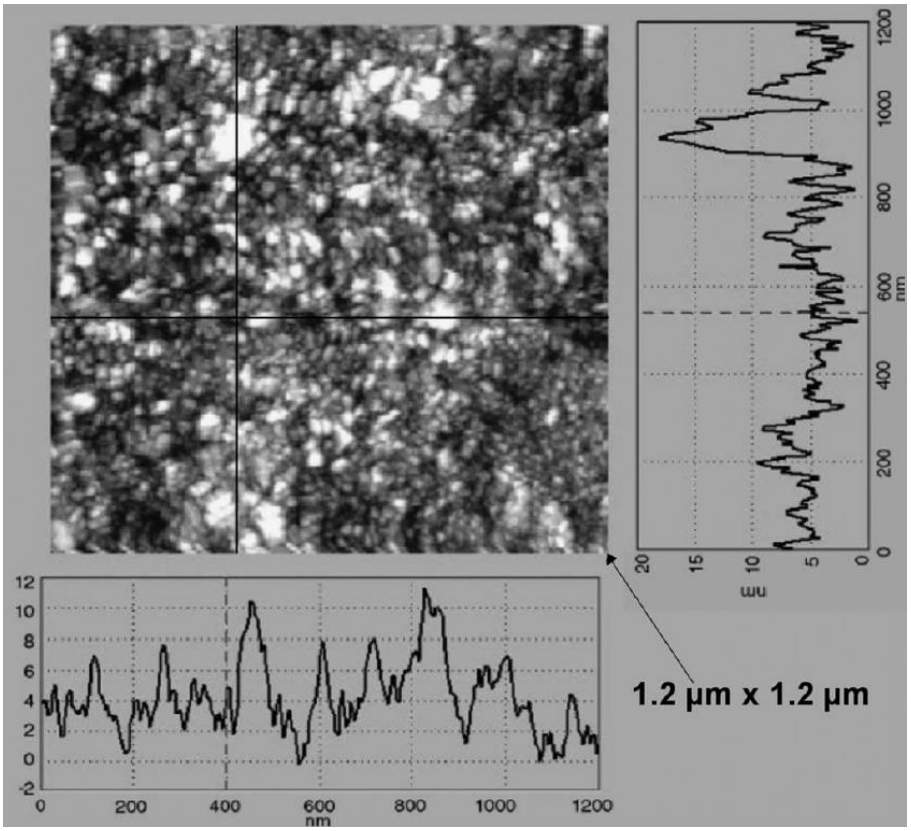

Fig. 7. STM surface line profile results on the glaze layer formed on Nimonic 80A at 0.314 m s^{-1} and 750 °C.

Nano-indentation (Table 2) indicates the glaze layers formed are of high hardness and high modulus, inferring a significant degree of hardening and also low levels of porosity in the glaze layers. The mean hardness value of 22.62 GPa is not too far removed from the theoretical hardness of bulk chromium oxide (Cr2O3) at 28.98 GPa [20].

3.2. Wear at 0.905 m s^{-1}

3.2.1. General observations—room temperature to 750 °C

Fig. 7 displays the wear data for the Nimonic 80A (sample)/Stellite 6 (counterface) system as a function of temperature under a load of 7 N at 0.905 m s^{-1} for a total sliding distance of 4522 m (the data for 0.314 m s^{-1} is also shown for comparison purposes). Weight losses at 0.905 m s^{-1} remained low only at room temperature (mean sample weight change K0.001(6) g) and 270 °C (weight change K0.000(4) g), coinciding with the presence of very fine loose oxide (300 nm to 1 mm in size) and a few isolated areas of compacted oxide on both the Nimonic 80A sample and Stellite 6 counterface wear surfaces (Fig. 8). As at 0.314 m s^{-1}, the presence of the loose oxide debris at 0.905 m s^{-1} prevented metal-to-metal contact and severe wear by metallic adhesion [3].

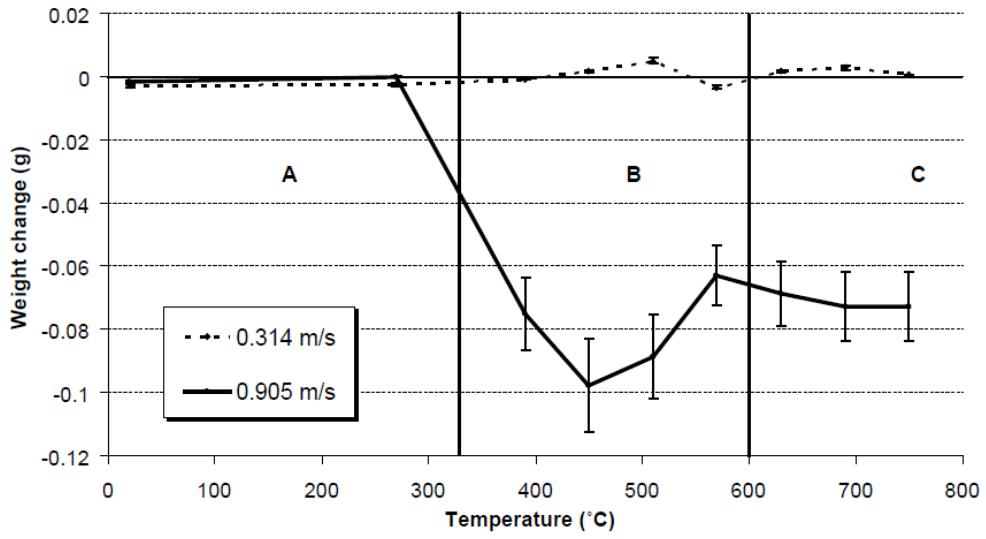

A. Loose oxide debris spread across wear surface, plus some compacted oxide formation (room temperature and 270°C)
B. Torn, metallic surface typical of adhesive wear, no traces of any oxide debris (390°C to 5 10°C) or only very limited oxide debris formation (570°C)
C. Loose oxide but with no compact oxide layers; fine parallel grooves in direction of sliding on Nimonic 80A surface (630°C to 750°C)
(Micrographs shown in Fig. 9)

Fig. 8. Weight change versus temperature for Nimonic 80A slid against Stellite 6 at 0.905 m s^{-1} (data for 0.314 m s^{-1} also shown).

However, at 0.905 m s^{-1} a transition was observed at 390 °C to a high weight loss (mean sample weight change K0.075(0)g - Fig. 7) severe 'metal-against-metal' wear regime

symptomatic of adhesive wear [3], accompanied by the production of high volumes of metallic debris and bright, highly damaged metallic wear surfaces on both the Nimonic 80A sample (Fig. 8) and Stellite 6 counterface (not shown). This high loss metallic severe wear regime was also present at 450 (weight change K0.097(8) g), 510 (weight change K0.088(7) g) and 570 8C (weight change K0.062(9) g). No oxide debris was observed between 390 and 510 °C and only a limited amount of oxide was observed at 570 °C; however, this oxide debris was insufficient to prevent metal-to-metal contact and severe wear continued. Although increasing temperature clearly increases the rate of oxidation, no glaze formation occurred due mainly to the low debris retention and low residence time of the debris on the Nimonic 80A surface.

A further wear transition was observed at 630 °C and 0.905 m s^{-1} to a high temperature oxidational wear regime, with continued high weight losses (weight change K0.068(4) g at 630 °C—Fig. 7). This wear regime was characterised by high levels of oxide debris generation and a smoother, heavily worn Nimonic 80A wear surface across which lay fine straight parallel grooves in the direction of sliding, covered by only a very thinly smeared layer of oxide (Fig. 8). Whilst the now high levels of oxide debris did prevent metal-to-metal contact and thus severe wear, there was no evidence of the oxide forming significant compact oxide layers. The fine, straight parallel grooves instead indicated the oxide was acting as an abrasive agent—hence material removal and wear remained high. Identical 'high weight loss by oxide abrasion' observations were made also at 690 (weight change K0.072(8) g) and 750 °C (weight change K0.079(8) g). Only on the Stellite 6 counterface was there a very limited development of glaze layers, accompanied by a reduction in wear related damage (not shown).

At 0.905 m s^{-1} as at 0.314 m s^{-1}, this paper concentrates on the wear observed at 750 °C.

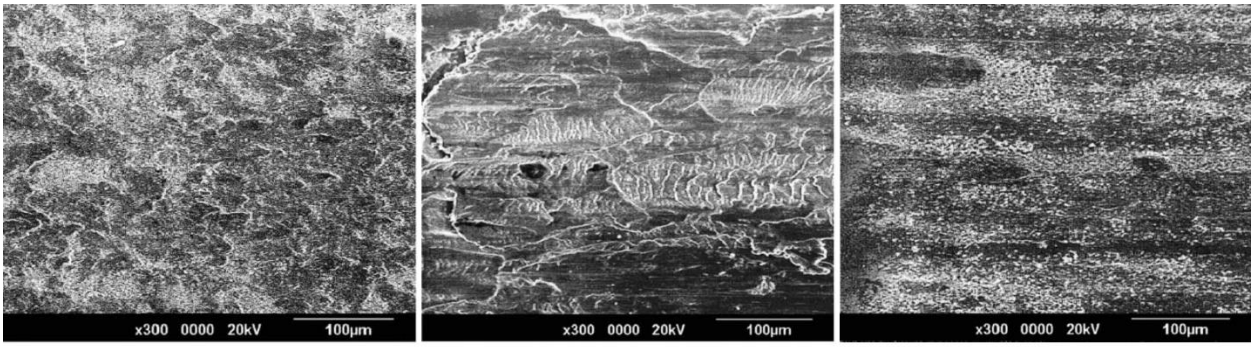

Fig. 9. SEM images of Nimonic 80A wear surfaces after sliding at 0.905 m s^{-1} (sliding distance 4522 m) against a Stellite 6 counterface at room temperature, 390 and 750 °C.

3.2.2. Wear at 750 °C (0.905 m s^{-1})

The coefficient of friction data measured during sliding at 750 °C (Fig. 9) demonstrated an initial unsettled 'run-in' period of high friction followed by a more settled 'steady state' period at 0.905 m s^{-1} as they had at 0.314 m s^{-1}. Values of friction at 0.905 m sK1 rose to as high as w0.73 during the run-in period before falling to between 0.33 and 0.51 during steady state sliding. Although friction values at 0.905 m s^{-1} during steady state were apparently lower than at 0.314m s^{-1} (where run-in friction was recorded at w0.7 and steady-state friction between 0.47 and 0.55), the variation in friction was greater (~20% at 0.905 m s^{-1}, ~12% at 0.314 m s^{-1}). It is possible that the higher variation in friction at 0.905 m s^{-1} may be attributable to the failure of the loose oxide

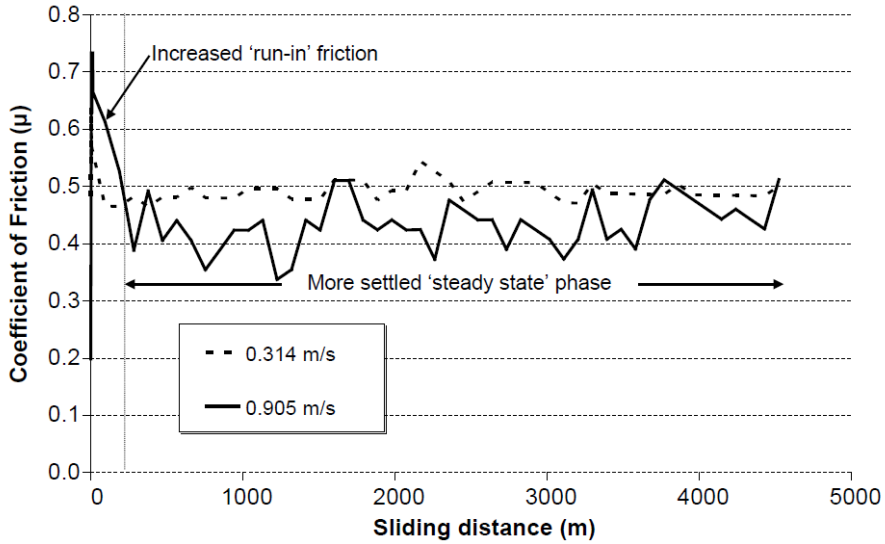

Fig. 10. Temperature versus coefficient of friction—Nimonic 80A versus Stellite 6 at 0.905 m sK1 and 750 8C (data for 0.314 m sK1 also shown).

debris formed to develop into comprehensive glaze layers on the Nimonic 80A sample surface. The parallel grooves on the Nimonic 80A wear surface indicated that at 750 8C (as at 630 and 690 8C) the oxide debris in fact assisted wear by abrasion, promoting the high weight losses observed from the Nimonic 80A sample (mean weight change K0.079(8) g).

EDX analysis of both the very fine oxide layer on the heavily worn Nimonic 80A wear scar and high quantities of loose oxide debris produced at 0.905 m s^{-1} indicated that the oxide generated was now dominated by nickel (~70 at.%) and chromium (~25 at.%) in proportions not too dissimilar to those present within the Nimonic 80A—no significant levels of Stellite 6-sourced cobalt were found. Also, a small amount of rough glaze removed from the wear scar of the Stellite 6 counterface was high in nickel (w68 at.%) and chromium (~25 at.%) with no trace of cobalt, indicating that in all cases the source of the oxide debris was the Nimonic 80A sample—there was little variation in these analyses. The dominant phases identified by XRD of the Nimonic 80A sample were a face-centred cubic Ni–Cr–Fe phase typical of the Nimonic 80A forming the sample and a very weak signal for NiO (from the very thinly smeared oxide layer). NiO and additionally Cr_2O_3 were dominant during XRD of the copious amounts of loose

debris—there was no evidence of any cobalt phases indicating absence of transfer from the Stellite 6 at 0.905 m s^{-1}.

4. Discussion

4.1. Wear at 0.314 m s^{-1}

The current data clearly indicates the rapid formation of a highly wear-protective glaze layer during high temperature sliding wear of the dissimilar interface Nimonic 80A/Stellite 6 (counterface) system at 0.314 m s^{-1} and 750 °C—the friction data (Fig. 4) shows only a brief period of unsettled run-in wear before low variability steady state sliding (with minimal further wear) was established. The high cobalt–chromium (34.2 at.% Co, 36.2 at.% Cr) and low nickel content (16.7 at.%) of the CoCr2O4 glaze layers formed on the Nimonic 80A samples suggest that in the Nimonic 80A/Stellite 6 system at 0.314m s^{-1}, wear predominantly occurred on the surface of the cobalt-rich Stellite 6 (Table 1). This wear during the initial run-in period was probably caused by a delamination type mechanism, due to low fatigue crack growth resistance and possible low fracture toughness of the Stellite 6 [3]. In addition, the ease of removal of material from the Stellite 6 potentially may be enhanced at higher sliding temperatures due to a phase transformation from hexagonal-close packed (as the primary constituent of Stellite 6 is cobalt) to face-centred-cubic [3]. The formation of a face-centred cubic phase within the Stellite 6 will have led to its easier (easy dislocation slip) deformation.

The debris generated was then transferred to the surface of the Nimonic 80A to form the glaze layer. Some intermixing with nickel-based debris removed from the Nimonic 80A also occurred, resulting in some location to- location variation in glaze composition—SAD conducted during TEM indicated the presence of NiO. The back transfer of some of this glaze to the Stellite 6 kept wear of the Stellite 6 counterface as well as the Nimonic 80A sample to very low levels.

The TEM and STM studies [3,19] indicate that the glaze layer formed is a nano-structured oxide—STM topography confirms the creation of nano-structures, showing a variation in grain size of between 5 and 10 nm (Fig. 10). These results together with the wear data demonstrate that such a nano-structure surface is highly effective in conferring high resistance to wear. The formation of nano-structured surfaces and the effectiveness of such surfaces in conferring improved wear resistance are the two main issues emerging from the work conducted on samples slid at 0.314 m s^{-1} and 750 °C, which require further discussion.

The work of various authors [13,21] indicates the generation of surfaces with ultra-fine structure in many systems during high temperature sliding wear. Mechanical mixing involving repeated welding, fracturing and rewelding of the debris generated from both contacting surfaces, is responsible for the generation of these ultra-fine structured surfaces. However, there has to date been little detailed investigation into the evolution of microstructures and defect structures generated accompanying the processes of high temperature sliding wear. Detailed TEM studies have allowed a greater understanding of the mechanisms of formation of wear resistant nano-structured surfaces.

As has been previously detailed [3,19,21], SEM, XRD and TEM analyses clearly show that the initial processes responsible for generating the glaze layer involve: (i) deformation of the surface, (ii) intermixing of the debris generated from the sample and the counterface surfaces, (iii) oxidation, (iv) further mixing and (v) repeated welding and fracture. These processes are aided by high temperature oxidation and diffusion. Positron annihilation studies confirmed the presence of vacancy clusters consisting of five vacancies [22].

The next step involves deformation of oxides and generation of dislocations leading to the formation of sub-grains. These sub-grains then undergo further refinement with increasing misorientation to give nano-structured grains with high angle boundaries (a process called 'fragmentation') resulting in a non-equilibrium state indicated by poorly defined and irregular grain boundaries. High internal stresses are created inside the grains - dislocation density and arrangement depends on the grain size; smaller grains contain fewer dislocations. The process leads to the formation of high-energy grain boundaries with a high defect density [23–27].

Measured values of micro-hardness for the glaze layers of no more than 6.06 GPa [3,19] indicated no Hall-Petch softening (a lowering of strength and hardness from that anticipated by the standard Hall-Petch relationship, that describes increased material strength and hardness as grain size is reduced [28]) despite the presence of nano-scale grains of size between 5 and 15 nm. In other words, no reduction in hardness attributable to very small nano-scale grain sizes was observed within the glaze layers. But it is to be additionally noted that the micro-hardness data [3,19] did not indicate any significant hardening of the surface layers either (the undeformed Nimonic 80A gave hardness values between 3.9 and 5.3 GPa).

However, during micro-hardness testing of the glaze layers, even at low loads, the indenter would at times readily penetrate or break up the glaze [3]—this implies higher glaze hardness levels than were measured during testing. Further investigation using nano-indentation did indicate a substantial degree of hardening (Table 2—mean hardness 22.62 GPa) [3], however, the use of nano-hardness data to interpret results needs to be treated with caution, due to vulnerability to localised variations in the glaze layer brought about by the extremely localised nature of nanoindentation.

Any such hardening can be attributed to the associated difficulties with dislocation generation in nano-sized grains [29,30] (as mentioned earlier, smaller grains contain fewer dislocations). As well as greater hardness, the presence of a nano-scale polycrystalline structure additionally infers improved fracture toughness on the glaze material. All of these factors make debris generation an inefficient process.

4.2. Wear at 0.905 m s^{-1}

At 0.905 m sK1, the rate of debris ejection was much greater than at 0.314 m s^{-1}. However, the extremely rapid generation of large amounts of Nimonic 80A-sourced NiO and Cr2O3 oxide debris at 750 8C and 0.905 m sK1 was great enough to overcome the high levels of debris ejection. Thus, debris residency was sufficient to prevent metal-to-metal contact at the Nimonic 80A/Stellite 6 wear interface (reflected by the lower friction values—Fig. 7), resulting in what was technically a mild wear regime.

However, the large amount of NiO and Cr2O3 debris did not form glaze (these oxides displayed a very low tendency to sinter and build up into oxide layers) on the Nimonic 80A wear surface and instead acted as agents to produce further wear by abrasion. The abrasive action of this debris resulted in the pattern of fine parallel wear grooves observed on the highly worn surface of the Nimonic 80A (Fig. 7). Even where glaze formation was observed on the Stellite 6 counterface surface from the NiO and Cr2O3, this glaze was abrasive in nature and promoted further wear of the Nimonic 80A surface—this abrasive mechanism is more effective at 750 8C due to significant thermal softening of Nimonic 80A.

The development of the limited glaze layer on the Stellite 6 counterface conversely protected the surface of the Stellite 6 from high levels of wear, with only a brief period of metal to- metal wear before the glaze layer formed (as indicated by the friction data—Fig. 7). This further supports the observation that the oxide debris generated at 750 8C is acting as an abrasive and enhancing the wear of the Nimonic 80A. The limited NiO/Cr2O3 glaze layer seals off the Stellite 6 surface, thus carbides present in the Stellite 6 surface cannot assist removal of material from the Nimonic 80A by ploughing .

In other studies [3], substitution of the nickel–chromium Nimonic 80A alloy with 99% purity Nickel 200e alloy as a sample material (i.e. Nickel 200^{TM} versus Stellite 6) under identical sliding conditions (0.905 m s^{-1}, 750 °C and 7 N load using a 'reciprocating-block-on-rotating-cylinder' configuration) resulted in the generation of only NiO debris. In the absence of Cr2O3, the Nickel 200^{TM}-sourced NiO debris rapidly formed highly wear protective glaze layers on the surfaces of both the Nickel 200e and Stellite 6 that resulted in negligible weight change. The development of this NiO glaze in the absence of Cr2O3 indicated that the Cr2O3 generated from Nimonic 80A during the current study acted as a promoter of wear and disrupted the process of glaze formation.

It is to be additionally observed that in the Nimonic80A/Stellite 6 (counterface) wear system at 0.314 m s^{-1},the oxides generated readily formed into wear-protective glaze layers—these included cobalt as well as nickel and chromium, which combined to give different phases to those seen at 0.905 m s^{-1}. At 0.314 m s^{-1}, the oxide phases generated included CoCr2O4 as well as some NiO and possibly a little Cr2O3—most of the chromium was incorporated into a combined oxide with cobalt that with NiO readily sintered together to form glaze layers. At0.905 m s^{-1}, the absence of cobalt transfer from the Stellite6 to the Nimonic 80A sample resulted in a complete absence of CoCr2O4, leaving behind only NiO and Cr2O3. The poor sintering characteristics in the presence of Cr2O3 in combination with increased oxide mobility at high sliding speed (0.905 m s^{-1}) have resulted in a loose oxide that enhances wear by abrasion.

The apparently poor sintering and glaze forming characteristics of NiO and Cr2O3 oxides generated from Nimonic 80A at 0.905 m s^{-1} appear at first to contradict the extensive studies carried out into glaze formation with Nimonic 80A-based systems [12,14–18]. However, such studies have been conducted using lower speed reciprocating sliding wear (a mean value for sliding speed of 83 mm sK1 is quoted) with a pin-on-disk configuration—such systems also have a higher degree of debris retention, in which the debris generated is less mobile and remains resident in the vicinity of the sliding surfaces. Thus, there is greater opportunity for the

oxide debris to sinter together to form glaze layers. In the current study, the 'block-on-cylinder' configuration is a unidirectional sliding wear system that especially at higher sliding speeds promotes debris mobility and ejection over retention. Whilst oxide debris is produced at high enough levels to prevent metal-to-metal contact, debris residency at the wear interface is insufficient to support glaze formation due to constant removal at 0.905 m s^{-1}. The reduced residency and greater mobility of the debris at 0.905 m s^{-1}does not allow sufficient contact time between debris particles for sintering and welding processes to occur that are necessary for glaze formation.

One issue that remains unresolved and is in need of further study is why is there a switch from greater wear of the Stellite 6 at 0.314 m s^{-1} to greater wear of the Nimonic80A at 0.905 m s^{-1}. This is not attributable to the 'blockon-cylinder' geometry favouring wear of either block(Nimonic 80A sample) or cylinder (Stellite 6 counterface)depending on sliding speed. On reversal of the sample and counterface during further studies under identical conditions(750 °C, 7 N load, sliding distance 4522 m) [3], Stellite 6still suffered greater damage as the sample at 0.314 m $s^{-1}$and Nimonic 80A underwent enhanced wear as the counterface at 0.905 m s^{-1}.

5. Summary

At 0.314 m sK1, the high temperature (750 °C) sliding wear of Nimonic 80A against Stellite 6 as a counterface alloy resulted in the rapid development of a wear resistant nano-structured Co/Cr/Ni oxide glaze layer. A process called 'fragmentation' involving deformation, generation of dislocations, formation of sub-grains and their increasing refinement causing increasing misorientation, was responsible for the formation of nano-structured grains. The improved wear resistance of such a layer has been attributed to the absence of Hall-Petch softening and enhanced fracture toughness of the surface.

At 0.905 m s^{-1}, sliding wear generated substantial quantities of Nimonic 80A-sourced NiO and Cr2O3 debris that did not readily form into glaze layers. Instead, the oxide acted as an abrasive agent and assisted the wear of the Nimonic 80A, a situation enhanced by a combination of high sliding speed (hence high debris mobility and low debris retention) and poor oxide sintering characteristics. In the current study, the presence of the Cr2O3 phase within the oxide debris appears to inhibit the sintering process—other studies [3] indicate that in the absence of Cr2O3, the NiO debris can readily sinter to form glaze layers.

Acknowledgements

Grateful acknowledgment is given to the UK Engineering Physics Science Research Council (EPSRC) and BritishGas for their financial support to this project.

References

[1] P.D. Wood. PhD Thesis. The effect of the counterface on the wear resistance of certain alloys at room temperature and 750 8C, Northumbria University, UK; 1997.

[2] S. Rose. PhD Thesis. Studies of the high temperature tribological behaviour of some superalloys, Northumbria University, UK; 2000.

[3] I.A. Inman. PhD Thesis. Compacted oxide layer formation under conditions of limited debris retention at the wear interface during high temperature sliding wear of superalloys, Northumbria University, UK; 2003.

[4] Stott FH, Lin DS, Wood GC. The structure and mechanism of formation of the “glaze” oxide layers produced on nickel-based alloys during wear at high temperatures. Corros Sci 1973;13:449–69.

[5] Johnson M, Moorhouse P, Nicholls JR. DTI industry valve project 1990;61–8.

[6] Aoh J-N, Chen J-C. On the wear characteristics of cobalt-based hardfacing layer after thermal fatigue and oxidation. Wear 2001;611: 250–1.

[7] Singh J, Alpas AT. Metall Mater Trans A 1996;27A:3135.

[8] Stott FH, Glascott J, Wood GC. Factors affecting the progressive development of wear-protective oxides on iron-base alloys during sliding at elevated temperatures. Wear 1984;97:93–106.

[9] Gee MG, Jennett NM. High resolution characterisation of tribochemical films on alumina. Wear 1995;193:133–45.

[10] Wood PD, Datta PK, Burnell-Gray JS, Wood N. Investigation into the high temperature wear properties of alloys contacting against different counterfaces. Mater Sci Forum 1997;251–254:467–74.

[11] Wisbey A, Ward-Close CM. Wear resistant surfaces on high temperature titanium alloy and titanium aluminide by diffusion bonding. Mater Sci Technol 1997;13:349–55.

[12] Jiang J, Stott FH, Stack MM. The effect of partial pressure of oxygen on the tribological behaviour of a nickel-based alloy, N80A, at elevated temperatures. Wear 1997;203–204:615–25.

[13] Li XY, Tandon KN. Microstructural characterization of mechanically mixed layer and wear debris in sliding wear of an Al alloy and an Al based composite. Wear 2000;245:148–61.

[14] Jiang J, Stott FH, Stack MM. A generic model for dry sliding wear of metals at elevated temperatures. Wear 2004;256:973–85.

[15] Jiang J, Stott FH, Stack MM. The role of triboparticulates in dry sliding wear. Tribology International 1998;31(5):245–56.

[16] Jiang J, Stott FH, Stack MM. Characterization of wear scar surfaces using combined three-dimensional topographic analysis and contact resistance measurements. Tribology International 1997;30(7):517–26.

[17] Jiang J, Stott FH, Stack MM. A mathematical model for sliding wear of metals at elevated temperatures. Wear 1995;181–183: 20–31.

[18] Jiang J, Stott FH, Stack MM. Some frictional features associated with the sliding wear of the nickel-base alloy N80A at temperatures to 250 8C. Wear 1994;176:185–94.

[19] Inman IA, Datta S, Du HL, Burnell-Gray JS, Pierzgalski S, Luo Q. Microscopy of glazed layers formed during high temperature sliding wear at 750 8C. Wear 2003;254:461–7.

[20] Brandes EA, Brook GB. Smithells metals reference book. 7th ed. London: Butterworth–Heinemann; 1992.

[21] Datta S, Inman I, Du HL, Luo Q. Microscopy of glazed layers formed during high temperature wear, Invited Talk at the Institute of Materials. Tribology Meeting, London; November 2001.

[22] Du HL, Datta PK, Inman IA, Kuzmann E, Suvegh K, Marek T, Ve´rtes A. Investigations of microstructures and defect structures in wear affected region created on Nimonic80A during high temperature wear. Tribology Letters 2005;18(3):393–402.

[23] Gleiter H. Nanocrystalline materials. Prog Mater Sci 1989;33: 223–315.

[24] Valiev RZ, Islamgalier RK, Alexandrov IV. Bulk nanostructured materials from severe plastic deformation. Prog Mater Sci 2000;45: 103–89.

[25] Lowe TC, Valiev RZ. Producing nanoscale microstructures through severe plastic deformation. JOM 2000;52:27–8.

[26] Ghosh AK, Huang W. Severe deformation based progress for grain subdivision and resulting microstructures. In: Lowe TC, Valiev RZ, editors. Investigations and applications of severe plastic deformation. Dordrecht: Kluwer Academic Publications; 2000. p. 29–36.

[27] Mishra RS, McFadden SX, Mukherjee AK. Analysis of tensile superplasticity in nanomaterials. Mater Sci Forum 1999;304–306:31–8.

[28] Morris DG. Mechanical behaviour of nanostructured materials. Trans-Tech Publications Ltd; 2000.

[29] Mishra RS, Mukherjee AK. Superplasticity in nanomaterials. In: Ghosh AK, Bieler TR, editors. Superplasticity and superplastic forming. Warrendale, PA: TMS; 1998. p. 109–16.

[30] Mishra RS, McFadden SX, Mukherjee AK. Tensile superplasticity in nanocrystalline materials produced by severe plastic deformation. In: Lowe TC, Valiev RZ, editors. Investigations and applications of severe plastic deformation. Dordrecht: Kluwer Academic Publications; 1994. p. 231–40.